# Synthesis and Photoresponse of Large GaSe Atomic Layers

Sidong Lei, Liehui Ge, Zheng Liu, Sina Najmaei, Gang Shi, Ge You, Jun Lou, Robert Vajtai, and Pulickel M. Ajayan*

Department of Mechanical Engineering and Materials Science, Rice University, Houston, Texas 77005, United States

S Supporting Information

ABSTRACT: We report the direct growth of large, atomically thin GaSe single crystals on insulating substrates by vapor phase mass transport. A correlation is identified between the number of layers and a Raman shift and intensity change. We found obvious contrast of the resistance of the material in the dark and when illuminated with visible light. In the photoconductivity measurement we observed a low dark current. The on−off ratio measured with a 405 nm at 0.5 mW/ mm^2 light source is in the order of 10^3; the photoresponsivity is 17 mA/W, and the quantum efficiency is 5.2%, suggesting possibility for photodetector and sensor applications. The photocurrent spectrum of few-layer GaSe shows an intense blue shift of the excitation edge and expanded band gap compared with bulk material.

KEYWORDS: 2D materials, atomically thin, gallium selenide, photoconductivity, vapor phase growth
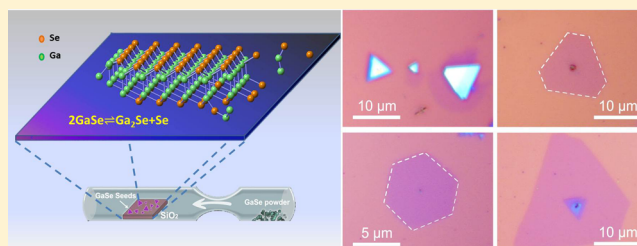
Since the discovery of graphene in 2004, two-dimensional (2D) materials have drawn increasing attention.[1] Graphene, as a single layer of hexagonally ordered carbon atoms, shows large electron and hole mobility value of 10^6 cm^2/ (Vs).[1−3] However, the absence of band gap limits the application in field effect transistors due to a low on/off current ratio[1] and results in challenges in building semiconductor logic circuits. In addition, the zero band gap structure in graphene also restricts the application of the material in the area of opto-electronics. Thus, a lot of efforts have been devoted to opening the band gap in order to improve the properties of graphene for these applications.[4−9] Alternatively, on the new frontiers in the field of 2D material research, various other layered materials that exhibit exciting properties such as h-BN,[10−12] MoS$_2$,[10,12,13] Bi$_2$Se$_3$,[14,15] Bi$_2$Te$_3$,[16,17] and so forth have been synthesized or isolated. Gallium selenide (GaSe) is a layered crystal widely used in the field of opto-electronics,[18] nonlinear optics, and terahertz experiments.[19−21] The band gap of bulk GaSe is about 2.0 eV.[22−24] There are several different crystal structures: β-GaSe, ε-GaSe, γ-GaSe, and so forth.[25] These crystal structures are generated from stacking the same fundamental GaSe layer building block, as shown in Figure 1a, although the stacking are different among them. Each layer of GaSe consists of four covalently bonded Se−Ga−Ga−Se atoms[23,25] with a D_{3h} symmetry[26] and has a lattice constant of 0.374 nm.[27] 2D GaSe has attracted interest from scientific community. Recently, good photoresponse and an on/off ratio of mechanically exfoliated GaSe have been reported.[28,29]

For device fabrication, large areas of single crystals are required, which is a challenge for exfoliation from bulk materials. Additionally, it is difficult to study the edge effect, because the lattice orientation of exfoliated layers is difficult to determine. Hence, the technique for growth of large area few-layer crystals of GaSe is important. To date, CVD growth of large area graphene,[30] h-BN,[31] MoS$_2$,[32] and so forth, has been developed. For GaSe, epitaxial growth has been demonstrated on the Si (111) surface as the lattice constant along a-axis of GaSe is only 2% less than the atomic spacing of Si (111) surface (3.84 nm). Extensive research has been conducted to understand the growth mechanism.[33−36] However, it is inconvenient to transfer the 2D crystal to an insulating substrate, and this entails difficulty in material characterization and device fabrication. As a consequence, it is beneficial to develop a method to grow 2D GaSe crystal directly on insulating substrates. Here, for the first time, we report a simple vapor phase mass transport (VMT) method for the synthesis of large area few atomic layer GaSe crystals on SiO$_2$ substrate. Its opto-electrical property is measured from devices fabricated directly on the growth substrate.

Large few-layer GaSe single crystals were synthesized by the VMT method, using grounded GaSe powder as a source and small GaSe flakes as seeds for crystal growth. Guided by the phase diagram of Ga−Se system,[37] the GaSe source and seeds were prepared with high-purity Ga$_2$Se$_3$ (99.99%, Alfa Aesar Company) and gallium (>99.99%, Sigma Aldrich Company). Ga$_2$Se$_3$ was grounded into powder and mixed with gallium at molar ratio of 1:1 and then sealed in an evacuated quartz tube under <10^{-3} Torr of argon. The mixture was heated to 950 °C in 2 h and kept at 950 °C for 1 h. Then the system was cooled down to 850 °C in 2 h followed by natural cooling. The
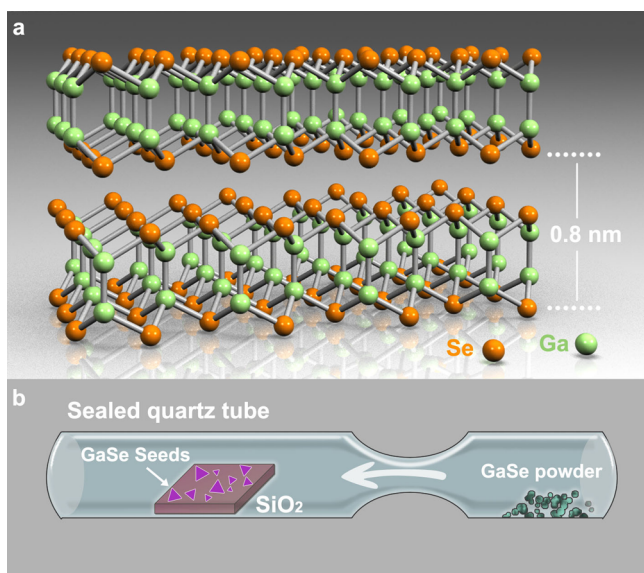
Figure 1. Schematics of the crystal structure of layered GaSe and the method of synthesis. (a) Two layers of GaSe are displayed where the selenium and gallium atoms are represented by orange and green spheres, respectively. The lattice constant along a axis is 0.374 nm and in the vertical direction is about 0.8 nm. (b) Quartz tube designed for the synthesis: a contraction at 15 cm from the right end separates the substrate (left) and source (right). During growth, the substrate with seeds is heated to 720 °C, and the GaSe powder is heated to 750 °C.

prepared samples have a diverse morphology, but most of them have triangular or hexagonal structures (see Supporting Information). Mica-like stacking is observed, which is an evidence of layered structures. To determine the elemental compositions of the crystals, energy dispersive X-ray spectra (EDX) were obtained from several spots of the crystals, and all of them gave an atomic ratio around 1:1 (see Supporting Information), suggesting a successful synthesis of GaSe in this process. The seeds for VMT growth were prepared by sonicating a small amount of micro GaSe crystals in isopropanol. The seeds were transferred onto a silicon wafer with 285 nm oxide layer which was cleaned with piranha solution before use. The rest of GaSe was ground into powder as an evaporation source. Then, the wafer with seeds on top and GaSe precursor were sealed in a quartz tube under vacuum ($<10^{-3}$ Torr of argon) as illustrated in Figure 1b. In a vacuum environment, the precursor is protected from oxidization, and its mean free path is large enough for mass transfer. The source and substrate were heated up to 750 and 720 °C respectively, for 20 min, followed by rapidly cooling to room temperature.

The optical images of GaSe crystals grown by VMT are shown in Figure 2a−d. Triangular, truncated triangular, and hexagonal crystals were observed. The crystal growth commonly starts from a nucleation site in center. The shape of the crystals transforms from triangles (Figure 2a) to truncated triangles (Figure 2b) as the distance from nucleation sites to the source increases. Although perfect hexagonal shapes are also observed, it is quite rare (Figure 2c). Large triangular flakes can be obtained when placing the substrate near to the source, and it is hard to control the growth process as it is very fast and the 2D crystal becomes multilayer quickly. On the contrary, the truncated ones grow much larger, and they are further away from the source. When the distance between the nucleation site and evaporation source becomes even larger, the

crystal loses the geometric symmetry (Figure 2d). The variation of shape could be explained by the change of concentration of source along the quartz tube. In the VMT process, the GaSe crystal decomposes into Se_2 and Ga_2Se which diffuse to the substrate independently,[33] and as their velocities and mean free paths are not the same, the ratio of the two species at the far end of the substrate deviates from 1:2. With the presence of nucleation centers, the two species recombine to form few-layer GaSe in lower temperature zones. The lack of one species impedes the growth of the crystal, as shown in Figure 2b, c, and d. Similarly, in the growth of MoS_2 atomic layers, the shape of the flakes transforms from triangles to hexagons as the concentration of sulfur decreases.[32]

Atomic force microscopy (AFM) is used to determine the thickness of the flakes. Figure 2e is the AFM height profile image of a complete piece of thin triangular flake with a nucleus in the center. The thickness of the flake measured along the dashed line in the AFM image is about 2 nm. The lattice constant of bulk GaSe along c-axis is about 1.6 nm,[27] which contains two layers of GaSe; that is, the distance between two neighboring layers is around 0.8 nm. This indicates that the 2D crystal consists of two or three layers of GaSe. Additionally, the surface of the crystal is very flat. This allows us to fabricate device directly on these samples without any material transfer which can compromise the material's quality.[12,38] The crystal structure of few-layer GaSe was characterized by transmission electronic microscopy (TEM). As shown in Figure 2f, the TEM micrograph and selected area electron diffraction (SAED) pattern show that the 2D GaSe crystal is of good quality. The lattice constant measured from the high-resolution TEM image along ⟨100⟩ direction is 0.36 nm, as demonstrated in the inset of Figure 2f. This value agrees with the reported value of a = 0.374 nm.[27]

The structure and quality of few-layer GaSe is further characterized by Raman spectroscopy. Single-layer GaSe has a D_{3h} symmetry. As a result, it has 12 vibrational modes: eight in-plane modes (E′ and E″), and four out-of-plane modes (A_1' and A_2'').[26,28,39] Except for the A_2'' mode, all the other modes are Raman active and significantly thickness-dependent. All Raman active modes are illustrated in Figure 3a. In our study, Raman spectra were obtained from 1 to 2 layer, few-layer, and thick flakes of GaSe which is shown is Figure 3b. Three peaks were observed in all spectra: one E^1_{1g} at 59 cm^{-1} (E″ mode for single layer) and two strong A_{1g} (A_1') modes at 132 cm^{-1} and 305 cm^{-1}, respectively. As the number of layers decreases, the relative intensity of the E^1_{1g} peaks decreases. This is the result of the reduction in the scattering centers for E_{1g} mode so the Raman scattering for this mode becomes less effective. The A_{1g} mode appears at 132 cm^{-1} in all samples. As the thickness approaches atomic scale, the intensity decreases significantly and even tends to vanish in 1−2 layers. The other A_{1g} mode at 305 cm^{-1} shows a red-shift when the number of layers is reduced. By fitting the peak with Lorentzian function (Figure 3c), it shifts from 305.2 cm^{-1} in bulk material to 303.4 cm^{-1} in single or double layer samples, which represents reduction of the force constant in the atomic layers as the sample becomes thinner. These observations are in agreement with those of mechanically exfoliated samples.[39] We did not observe any peak for E_{2g} mode at 208 cm^{-1} in thin samples. However, a peak appears at 230 cm^{-1} in single or double layer samples and shifts to 227 cm^{-1} in thicker, few-layer samples. There are two possible reasons for this peak: (a) it is shifted from E_{2g} located at 208 cm^{-1} in bulk sample and two; (b) it is originated from
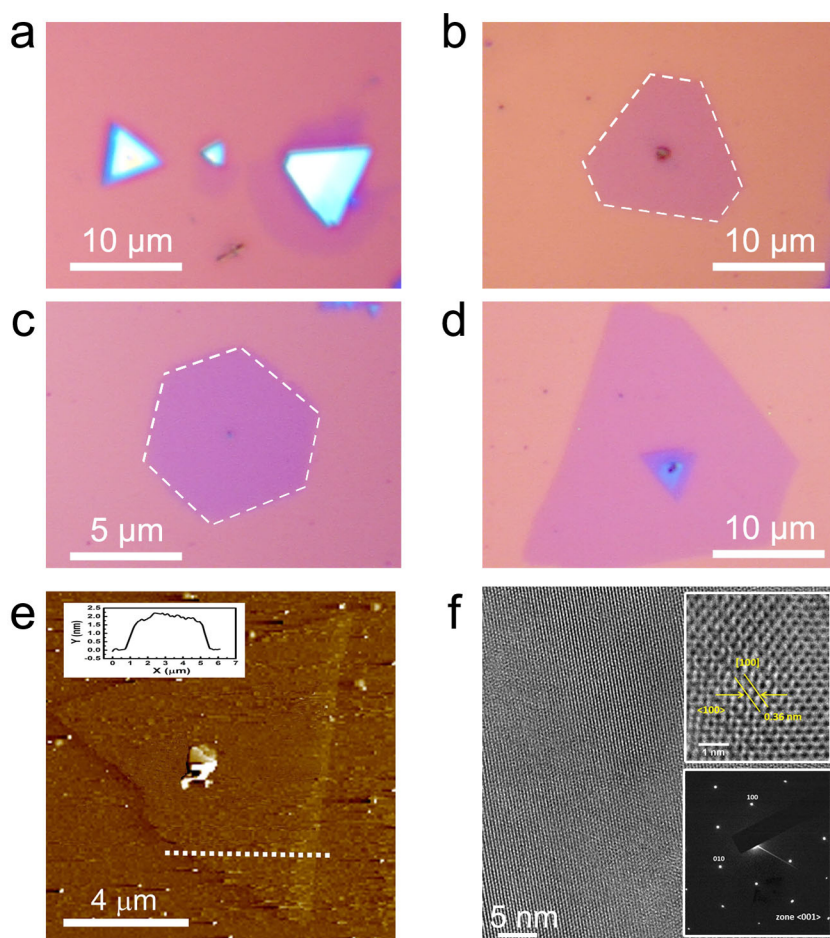
Figure 2. Topology of layered GaSe. (a−d) Optical images of GaSe flakes and seeds on a Si wafer coated by thermal oxide. The shape of the flakes transforms from triangle to truncated triangle and finally loses the geometric symmetry with increasing source to substrate distance: (a) multilayered triangular, (b) truncated triangular, one to three layer thickness, (c) hexagonal, (d) larger area flake with imperfect geometry. (e) AFM image of a triangular GaSe flake. The thickness is 2.0 nm (left upper corner inset) so this flake has one to three layers of GaSe. (f) TEM, HRTEM images, and electron diffraction pattern of a GaSe flake. The lattice spacing of [100] plane is measured along ⟨100⟩ and shows a value of 0.36 nm, literature value for the bulk crystal is 0.374 nm. The electron diffraction pattern is taken with a beam parallel to the ⟨001⟩ direction.

another weak E^2_{1g} mode in bulk material. A previous study shows that the E^2_{1g} mode becomes more intense as the number of layers decreases,[39] and it possibly comes from this mode and experiences a red shift due to the interaction with the substrate which does not exist in bulk. Generally, the relationship between Raman scattering and the number of layers agrees very well with the exfoliated samples, which indicates that the VMT grown samples have similar quality to the exfoliated ones.

Bulk GaSe is widely used for photodetector and nonlinear optics. So it is important to probe the photoresponse of the VMT grown GaSe layers here. To characterize the photoresponse, dark current and photocurrent from a 2D crystal of 6−8 layers are measured with Ti/Au electrodes in a two-probe setting. The photocurrent is measured with 0.5 mW/mm^2 405 nm laser excitation as shown in Figure 4a. In contrast to previous studies in photoresponse of the mechanically exfoliated samples,[28,29] the dark current of the sample is extremely low in the order of pA. The bulk GaSe synthesized from gallium and selenium is a p-type semiconductor; the impurity in the crystal causes large charge carrier density, ∼ $10^{15}-10^{16}$ cm^{-3}.[23,40] As a result, large dark currents in bulk and exfoliated GaSe are observed. The lower dark current may indicates that the VMT grown sample has lower carrier density, that is, lower impurity density. The on−off ratio of VMT grown

GaSe is high. When 10 V bias is applied to the sample, the photocurrent is about 3 orders larger than the dark current. Photoresponsivity or photocurrent generation efficiency is the ratio of generated photocurrent and incident optical power. It is a critical parameter to evaluate the performance of the photodetectors. For our device, the photoresponsivity is 17 mA/W, and the quantum efficiency is 5.2% with a bias of 10 V and an excitation wavelength of 405 nm. These values are much better than layered MoS_2 which has a photoresponsivity in the order of 1 mA/W.[13] The extremely low dark current and high photoresponse make VMT grown GaSe few-layer material more favorable for photodetector and sensor applications because lower dark current and high photoresponsivity help to increase the signal-to-noise ratio in such devices.

Photoresponse wavelength is another critical factor for photoelectronic materials and devices. The photocurrent spectrum was recorded from 350 to 750 nm. The excitation light was chopped at 177 Hz, and current was measured with a lock-in amplifier. The photocurrent spectrum obtained from a crystal of 6−8 layers is shown in Figure 4b. There is a sharp peak at 380 nm which corresponds to an energy gap of 3.3 eV. Besides this peak, there is a tail that extends to 620 nm. In bulk crystal, 620 nm corresponds to a band gap of 2.0 eV.[24] Generally, in a layered semiconductor, the band gap increases
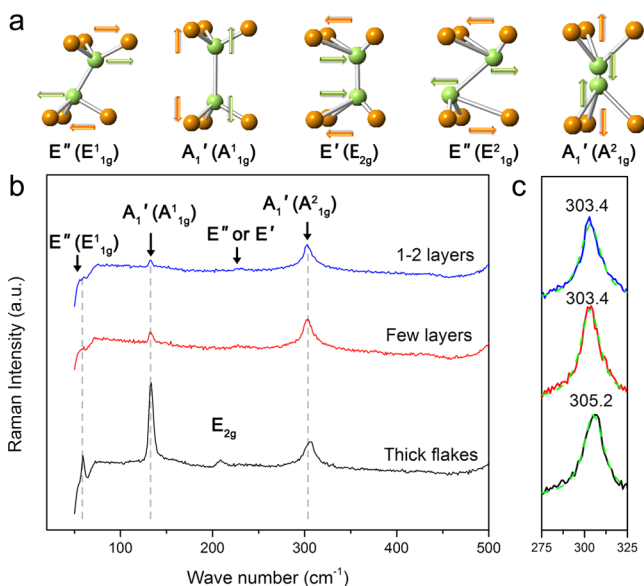
Figure 3. Raman spectra of layered GaSe with various thickness. (a) Schematics of the Raman modes of GaSe. The colored arrows designate the vibrational directions of selenium atoms (orange) and gallium (green) atoms. (b) Raman spectra of 1−2 layers (blue), few layers (red), and thick flakes (black) of GaSe. The intensities of the spectra are normalized and shifted vertically for easier reading. With the decreasing number of layers the intensities of E^1_{1g} mode at 59 cm^{-1} and A_{1g} mode at 132 cm^{-1} decrease, the E_{2g} mode at 208 cm^{-1} diminishes, and a weak peak at 230 cm^{-1} appears. (c) The A_{1g} peak at 305.2 cm^{-1} shifts to 303.4 cm^{-1} in 1−2 layers and a few layers of GaSe.

as the number of layers approaches atomic dimensions. For example, the band gap of MoS$_2$ changes from 1.2 eV in bulk to 1.8 eV in a single layer.[32] In GaSe, the band gap changes more dramatically which is predicted by theoretical calculation. It is shown by experiments[25] that the mechanism for this dramatic change in band gap is the existence of three-dimensional electronic interactions in GaSe in addition to van de Waals interaction in other types of layered materials such as graphene. In GaSe, the top of the valence band is mainly formed by a p$_z$-like orbit from the Se atoms. Deeper in the valence band, there

are p$_x$ and p$_y$-like orbits which contribute to an interband transition with an energy around 3.2 eV, shown in Figure 4f.[41] The overlap of p$_z$ orbits of Se atoms[27] leads to a more intense interlayer interaction and energy level splitting which significantly narrow the band gap in bulk GaSe. When the number of layer is reduced, this coupling becomes weaker and effective density of state is reduced so that the absorption in the range from 400 to 620 nm is measurably weakened. Instead, p$_x$ and p$_y$-like orbits are in-plane electronic states which are not effected by nearby layers as much, so the reduction of number of layers does not change the 3.3 eV transition.

In summary, we demonstrated here a vapor-phase mass transport method for large-area few-layer GaSe crystal growth directly on insulating substrates. The AFM and TEM results confirm that few-layer high quality GaSe single crystals as large as tens of micrometers have been synthesized. The Raman study reveals the relationship between number of GaSe layers and Raman shift and intensity. The results are similar to mechanically exfoliated samples. In the photocurrent measurement, an evident electrical photoresponse and a low dark current were observed. The on−off ratio is in the order of 10^3. The photoresponsivity is 17 mA/W, and the quantum efficiency is 5.2%. 2D GaSe crystal is a promising material for application in photodetectors due to the low dark current and high on−off ratio. The photocurrent spectra show an intense blue shift of the excitation edge and expanded band gap due to a weaker p$_z$-like orbit interaction as the number of layer decreases. This provides clues to modulate the electronic orbital structure of the few-layer GaSe material for optoelectronics and optical applications.

■ ASSOCIATED CONTENT

ⓈSupporting Information

SEM images and EDX spectrum of the GaSe microcrystals. This material is available free of charge via the Internet at http://pubs.acs.org.

■ AUTHOR INFORMATION

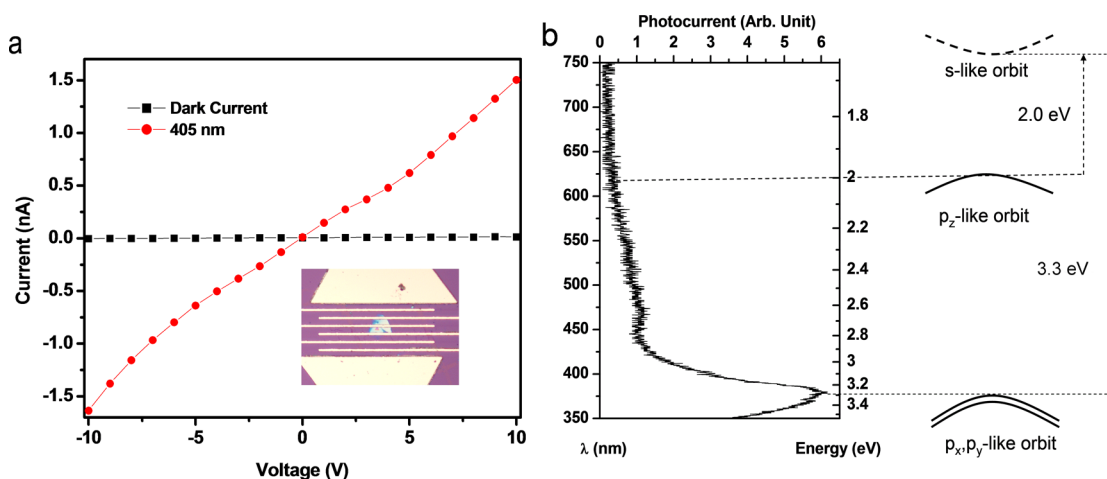**Corresponding Author**
*E-mail: ajayan@rice.edu.

Figure 4. Photoresponse of a GaSe crystal consisting of 6−8 layers. (a) Dark current (black) and the photocurrent (red), the latter is measured with a 0.5 mW/mm^2 intensity, 405 nm wavelength; the photoresponsivity is 17 mA/W, and the quantum efficiency is 5.2%. (b) The photocurrent spectrum and the corresponding energy level structures.[41] The peak at 3.3 eV corresponds to the transition from p$_x$ and p$_y$-like orbits to the conduction band and the tail extending to 2.0 eV corresponds to the transition from the p$_z$-like orbit to the conduction band.

Notes

The authors declare no competing financial interest.

■ REFERENCES

(1) Novoselov, K. S.; Geim, A. K.; Morozov, S. V.; Jiang, D.; Zhang, Y.; Dubonos, S. V.; Grigorieva, I. V.; Firsov, A. A. *Science* **2004**, *306* (5696), 666−669.

(2) Schwierz, F. *Nat. Nanotechnol.* **2010**, *5* (7), 487−496.

(3) Chen, J. H.; Jang, C.; Xiao, S.; Ishigami, M.; Fuhrer, M. S. *Nat. Nanotechnol.* **2008**, *3* (4), 206−209.

(4) Li, X.; Wang, X.; Zhang, L.; Lee, S.; Dai, H. *Science* **2008**, *319* (5867), 1229−1232.

(5) Zhou, S. Y.; Gweon, G. H.; Fedorov, A. V.; First, P. N.; de Heer, W. A.; Lee, D. H.; Guinea, F.; Castro Neto, A. H.; Lanzara, A. *Nat. Mater.* **2007**, *6* (10), 770−775.

(6) Hicks, J.; Tejeda, A.; Taleb-Ibrahimi, A.; Nevius, M. S.; Wang, F.; Shepperd, K.; Palmer, J.; Bertran, F.; Le Fèvre, P.; Kunc, J.; de Heer, W. A.; Berger, C.; Conrad, E. H. *Nat. Phys.* **2012**, *9* (1), 49−54.

(7) Fan, X.; Shen, Z.; Liu, A. Q.; Kuo, J. L. *Nanoscale* **2012**, *4* (6), 2157−2165.

(8) Shinde, P.; Kumar, V. *Phys. Rev. B* **2011**, *84* (12), 125401.

(9) Usachov, D.; Vilkov, O.; Gruneis, A.; Haberer, D.; Fedorov, A.; Adamchuk, V. K.; Preobrajenski, A. B.; Dudin, P.; Barinov, A.; Oehzelt, M.; Laubschat, C.; Vyalikh, D. V. *Nano Lett.* **2011**, *11* (12), 5401−5407.

(10) Coleman, J. N.; Lotya, M.; O'Neill, A.; Bergin, S. D.; King, P. J.; Khan, U.; Young, K.; Gaucher, A.; De, S.; Smith, R. J.; Shvets, I. V.; Arora, S. K.; Stanton, G.; Kim, H. Y.; Lee, K.; Kim, G. T.; Duesberg, G. S.; Hallam, T.; Boland, J. J.; Wang, J. J.; Donegan, J. F.; Grunlan, J. C.; Moriarty, G.; Shmeliov, A.; Nicholls, R. J.; Perkins, J. M.; Grieveson, E. M.; Theuwissen, K.; McComb, D. W.; Nellist, P. D.; Nicolosi, V. *Science* **2011**, *331* (6017), 568−571.

(11) Alem, N.; Erni, R.; Kisielowski, C.; Rossell, M.; Gannett, W.; Zettl, A. *Phys. Rev. B* **2009**, *80* (15), 155425.

(12) Lee, C.; Li, Q.; Kalb, W.; Liu, X. Z.; Berger, H.; Carpick, R. W.; Hone, J. *Science* **2010**, *328* (5974), 76−80.

(13) Yin, Z.; Li, H.; Jiang, L.; Shi, Y.; Sun, Y.; Lu, G.; Zhang, Q.; Chen, X.; Zhang, H. *ACS Nano* **2012**, *6* (1), 74−80.

(14) Zhang, J.; Peng, Z.; Soni, A.; Zhao, Y.; Xiong, Y.; Peng, B.; Wang, J.; Dresselhaus, M. S.; Xiong, Q. *Nano Lett.* **2011**, *11* (6), 2407−2414.

(15) Hong, S. S.; Kundhikanjana, W.; Cha, J. J.; Lai, K.; Kong, D.; Meister, S.; Kelly, M. A.; Shen, Z. X.; Cui, Y. *Nano Lett.* **2010**, *10* (8), 3118−3122.

(16) Teweldebrhan, D.; Goyal, V.; Balandin, A. A. *Nano Lett.* **2010**, *10* (4), 1209−1218.

(17) Teweldebrhan, D.; Goyal, V.; Rahman, M.; Balandin, A. A. *Appl. Phys. Lett.* **2010**, *96* (5), 053107.

(18) Leontie, L.; Evtodiev, I.; Nedeff, V.; Stamate, M.; Caraman, M. *Appl. Phys. Lett.* **2009**, *94* (7), 071903.

(19) Shi, W.; Ding, Y. J.; Fernelius, N.; Vodopyanov, K. *Opt. Lett.* **2002**, *27* (16), 1454.

(20) Allakhverdiev, K. R.; Yetis, M. Ö.; Özbek, S.; Baykara, T. K.; Salaev, E. Y. *Laser Phys.* **2009**, *19* (5), 1092−1104.

(21) Kübler, C.; Huber, R.; Tübel, S.; Leitenstorfer, A. *Appl. Phys. Lett.* **2004**, *85* (16), 3360.

(22) Le Toullec, R.; Balkanski, M.; Besson, J. M.; Kuhn, A. *Phys. Lett. A* **1975**, *55* (4), 245−246.

(23) Bube, R.; Lind, E. *Phys. Rev.* **1959**, *115* (5), 1159−1164.

(24) Alekperov, O. Z.; Godjaev, M. O.; Zarbaliev, M. Z.; Suleimanov, R. A. *Solid State Commun.* **1991**, *77* (1), 65−67.

(25) Plucinski, L.; Johnson, R.; Kowalski, B.; Kopalko, K.; Orlowski, B.; Kovalyuk, Z.; Lashkarev, G. *Phys. Rev. B* **2003**, *68* (12), 125304.

(26) Wieting, T.; Verble, J. *Phys. Rev. B* **1972**, *5* (4), 1473−1479.

(27) Rybkovskiy, D.; Arutyunyan, N.; Orekhov, A.; Gromchenko, I.; Vorobiev, I.; Osadchy, A.; Salaev, E. Y.; Baykara, T.; Allakhverdiev, K.; Obraztsova, E. *Phys. Rev. B* **2011**, *84* (8), 085314.

(28) Hu, P.; Wen, Z.; Wang, L.; Tan, P.; Xiao, K. *ACS Nano* **2012**, *6* (7), 5988−5994.

(29) Late, D. J.; Liu, B.; Luo, J.; Yan, A.; Matte, H. S.; Grayson, M.; Rao, C. N.; Dravid, V. P. *Adv. Mater.* **2012**, *24* (26), 3549−3554.

(30) Kim, K. S.; Zhao, Y.; Jang, H.; Lee, S. Y.; Kim, J. M.; Ahn, J. H.; Kim, P.; Choi, J. Y.; Hong, B. H. *Nature* **2009**, *457* (7230), 706−710.

(31) Song, L.; Ci, L.; Lu, H.; Sorokin, P. B.; Jin, C.; Ni, J.; Kvashnin, A. G.; Kvashnin, D. G.; Lou, J.; Yakobson, B. I.; Ajayan, P. M. *Nano Lett.* **2010**, *10* (8), 3209−3215.

(32) Najmaei, S.; Liu, Z.; Zhou, W.; Zou, X.; Shi, G.; Lei, S.; Yakobson, B. I.; Idrobo, J.-C.; Ajayan, P. M.; Lou, J. *arXiv:1301.2812*.

(33) Ludviksson, A.; Rumaner, L. E.; Rogers, J. W.; Ohuchi, F. S. *J. Cryst. Growth* **1995**, *151* (1−2), 114−120.

(34) Vinh, L. T.; Eddrief, M.; Sébenne, C.; Sacuto, A.; Balkanski, M. *J. Cryst. Growth* **1994**, *135* (1−2), 1−10.

(35) Zheng, Y.; Koëbel, A.; Pétroff, J. F.; Boulliard, J. C.; Capelle, B.; Eddrief, M. *J. Cryst. Growth* **1996**, *162* (3−4), 135−141.

(36) Palmer, J. E.; Saitoh, T.; Yodo, T.; Tamura, M. *J. Appl. Phys.* **1993**, *74* (12), 7211.

(37) Gouskov, A.; Camassel, J.; Gouskov, L. *Prog. Crystal Growth Charact.* **1982**, *5* (4), 323−413.

(38) Choi, J. S.; Kim, J. S.; Byun, I. S.; Lee, D. H.; Lee, M. J.; Park, B. H.; Lee, C.; Yoon, D.; Cheong, H.; Lee, K. H.; Son, Y. W.; Park, J. Y.; Salmeron, M. *Science* **2011**, *333* (6042), 607−610.

(39) Late, D. J.; Liu, B.; Matte, H. S. S. R.; Rao, C. N. R.; Dravid, V. P. *Adv. Funct. Mater.* **2012**, *22* (9), 1894−1905.

(40) Augelli, V.; Manfredotti, C.; Murri, R.; Vasanelli, L. *Phys. Rev. B* **1978**, *17* (8), 3221−3226.

(41) Segura, A.; Bouvier, J.; Andres, M. V.; Manjon, F. J.; Munoz, V. *Phys. Rev. B* **1997**, *56* (7), 4075−4084.